Acute Nitric Oxide Synthase Inhibition Accelerates Transendothelial Insulin Efflux In Vivo

Ian M. Williams,[1] P. Mason McClatchey,[1] Deanna P. Bracy,[1,2] Francisco A. Valenzuela,[3] and David H. Wasserman[1,2]

Diabetes 2018;67:1962–1975 | https://doi.org/10.2337/db18-0288

METABOLISM

Before insulin can stimulate glucose uptake in muscle, it must be delivered to skeletal muscle (SkM) through the microvasculature. Insulin delivery is determined by SkM perfusion and the rate of movement of insulin across the capillary endothelium. The endothelium therefore plays a central role in regulating insulin access to SkM. Nitric oxide (NO) is a key regulator of endothelial function and stimulates arterial vasodilation, which increases SkM perfusion and the capillary surface area available for insulin exchange. The effects of NO on transendothelial insulin efflux (TIE), however, are unknown. We hypothesized that acute reduction of endothelial NO would reduce TIE. However, intravital imaging of TIE in mice revealed that reduction of NO by L-N^G-nitro-L-arginine methyl ester (L-NAME) enhanced the rate of TIE by ∼30% and increased total extravascular insulin delivery. This accelerated TIE was associated with more rapid insulin-stimulated glucose lowering. Sodium nitroprusside, an NO donor, had no effect on TIE in mice. The effects of L-NAME on TIE were not due to changes in blood pressure alone, as a direct-acting vasoconstrictor (phenylephrine) did not affect TIE. These results demonstrate that acute NO synthase inhibition increases the permeability of capillaries to insulin, leading to an increase in delivery of insulin to SkM.

The microvasculature is an important regulator of insulin action in skeletal muscle (SkM), as it controls the delivery of insulin and glucose to myocytes (1–5). Insulin delivery to SkM is determined by both muscle perfusion (2) and, subsequently, movement of insulin across the continuous endothelium of SkM capillaries into the interstitial space (6). The capillary walls in SkM are a significant barrier that restricts insulin's access to the myocyte (4,5). As such, the rate of transendothelial insulin efflux (TIE) is a major determinant of insulin delivery to and action in SkM (7,8). Given this key role of the endothelium in regulating insulin delivery to SkM, endothelial function is an important variable that regulates insulin action in SkM.

Endothelial function emerges from the complex interaction of hemodynamic forces, cell-cell interactions, and a myriad of biochemical signals. One signaling molecule that is particularly important for endothelial function is nitric oxide (NO), which regulates several vascular functions including vasoactivity and microvascular permeability (9). Three different NO synthase (NOS) isoforms (endothelial, inducible, and neuronal) can produce NO, oxidizing L-arginine to generate L-citrulline and NO (9). NO then imparts biological activity by covalently bonding to cysteine or heme residues on proteins and altering their function (10). Under normal conditions, NO promotes vasodilation and maintains endothelial barrier function. However, when the bioavailability of NO is reduced, the endothelium becomes inflamed and displays abnormal vasoreactivity (11).

Reduced endothelial NO bioavailability and endothelial dysfunction have been strongly correlated with insulin resistance (12). Obese, insulin-resistant humans have an impaired response to endothelium-dependent vasodilators (13), indicating that they have reduced NO bioavailability. Furthermore, the ability of insulin to activate endothelial NOS (eNOS) in endothelial cells (ECs) is impaired in mouse models of obesity and insulin resistance (14). Conversely, drugs that act on the renin-angiotensin system to enhance endothelial function and increase NO bioavailability improve glucose homeostasis (15,16). These

[1]Department of Molecular Physiology and Biophysics, Vanderbilt University, Nashville, TN
[2]Mouse Metabolic Phenotyping Center, Vanderbilt University, Nashville, TN
[3]Lilly Research Laboratories, Indianapolis, IN
Corresponding author: Ian M. Williams, ian.m.williams@vanderbilt.edu.

Received 8 March 2018 and accepted 3 July 2018.

This article contains Supplementary Data online at http://diabetes.diabetesjournals.org/lookup/suppl/doi:10.2337/db18-0288/-/DC1.

observations suggest that insulin resistance in SkM may be linked mechanistically to reduced endothelial NO bioavailability.

Endothelial NO bioavailability may directly regulate insulin delivery to and action in SkM by modulating either SkM perfusion or TIE. Several groups have demonstrated that pharmacological reduction of NO during steady-state hyperinsulinemia diminishes perfusion and glucose uptake in SkM in both humans and rodents (14,17–20). Furthermore, mice lacking eNOS display peripheral insulin resistance and impaired SkM perfusion (21,22). These findings demonstrate that reduction of endothelial NO can limit SkM perfusion and steady-state, insulin-stimulated glucose uptake in muscle. Whether impaired TIE contributes to the effects of reduced NO remains to be explored.

With respect to TIE, Barrett and colleagues (23) showed that NO promotes the uptake of fluorescently labeled insulin into cultured bovine aortic ECs. That study should be interpreted with caution, however, as we demonstrated that the mechanism of TIE in vivo is different than that in cultured ECs (6,24,25). In vivo, TIE is accomplished through a fluid-phase transport mechanism that is nonsaturable and does not involve the insulin receptor (6), whereas cultured ECs take up insulin through a saturable, insulin receptor–mediated process (24). In addition, several in vivo studies have shown that pharmacological inhibition of NOS increases microvascular permeability (reviewed by Kvietys and Granger [26]). Thus, the effect of varying endothelial NO levels on the movement of insulin across the SkM capillary endothelium in vivo remains unclear.

In this study we assessed the effects of acutely modulating NO levels on TIE using an intravital microscopy technique we recently developed (6). We show that reduction of NO levels through acute inhibition of NOS with L-N^G-nitro-L-arginine methyl ester (L-NAME) increases TIE, enhances total extravascular insulin delivery, and accelerates insulin-induced glucose lowering in vivo. Furthermore, these effects of L-NAME seem to be mediated by eNOS and are not due to changes in blood pressure (BP) alone. The NO donor sodium nitroprusside (SNP), on the other hand, has no effect on TIE kinetics in mice. Thus, in contrast to its inhibitory effects on SkM perfusion, acute pharmacological reduction of endothelial NO increases the permeability of SkM capillaries to insulin in vivo and enhances total extravascular insulin delivery.

RESEARCH DESIGN AND METHODS

Mice

For all experiments, we used 9- to 15-week-old male C57Bl/6J mice (The Jackson Laboratory) fed a standard chow diet (5001 Laboratory Rodent; LabDiet). Age-matched mice were used for direct comparisons. Mice were housed in a temperature- and humidity-controlled facility and maintained under a 12-h light/12-h dark cycle. Mice were deprived of food for 5 h before all experiments. Studies were approved by the Vanderbilt University Institutional Animal Care and Use Committee.

Catheterization

The carotid artery and jugular vein were catheterized as described previously (27). Only jugular vein catheters were implanted for intravital microscopy studies. Both the carotid artery and jugular vein were catheterized for insulin tolerance tests and BP experiments.

Treatment Protocols

To determine how acutely modulating NO and BP affects TIE and glucose metabolism, mice were treated with either L-NAME (a nonspecific NOS inhibitor), *S*-methyl-L-thiocitrulline (SMTC; a neuronal NOS [nNOS] inhibitor), SNP (an NO donor), phenylephrine, or hydralazine (Sigma-Aldrich). Phenylephrine and hydralazine act directly on smooth muscle to raise and lower BP, respectively (28,29). The same protocols were used for intravital microscopy, BP measurements, and insulin tolerance experiments in mice receiving each drug treatment. For the L-NAME experiment, mice were administered a 30 mg/kg i.v. bolus (50-μL volume) of L-NAME or an equivalent volume of saline 15 min before the experiments started (Fig. 1*A*). This timing and dose of L-NAME were chosen because they were previously shown to increase BP (i.e., inhibit NOS) in rats (30). To selectively inhibit nNOS, mice were administered a 0.56 μg/kg bolus of SMTC. This dose has been shown to selectively inhibit nNOS without altering eNOS activity in rats (31–33). For SNP experiments, mice were treated with a continuous infusion of either SNP (100 μg/kg/min) or saline beginning 15 min before the experiment and continuing throughout the course of the study (Supplementary Fig. 6*A*). This dose was chosen on the basis of a previous study that showed that a 37 μg/kg/min infusion lowered BP within 15 min (34). We increased this dose to ensure that SNP would be effective in anesthetized mice. Phenylephrine and hydralazine were administered as primed, continuous infusions starting 5 min before the experiments and continuing throughout the study (Supplementary Fig. 9*A*). Mice were given a 300 μg/kg bolus followed by a 300 μg/kg/min continuous infusion of phenylephrine, or a 1 mg/kg bolus followed by a 1 mg/kg/min continuous infusion of hydralazine. These doses were chosen based on their ability to raise (phenylephrine) or lower (hydralazine) BP (35,36). Control mice were treated with saline administered at equivalent infusion rates and volumes.

Intravital Microscopy

Insulin labeled with Alexa Fluor 647 (INS-647) was imaged in vivo in the mouse gastrocnemius as recently described (6). Mice were anesthetized with a ketamine/xylazine/acepromazine cocktail, and the gastrocnemius was carefully exposed by trimming away skin and fascia. Mice were situated on a custom stage mount, and the exposed gastrocnemius was continuously superfused with a bicarbonate-buffered (18 mmol/L) physiological saline solution

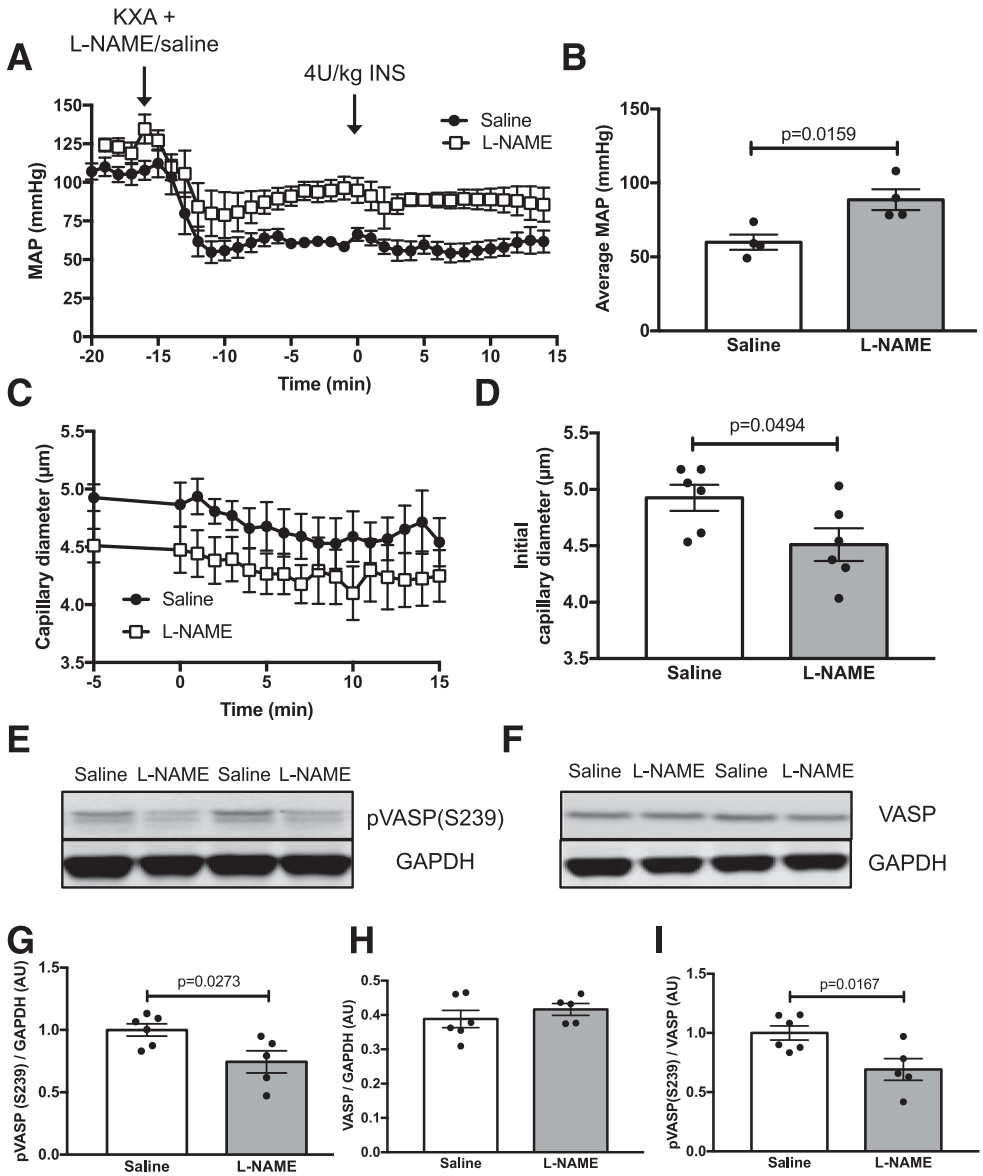

Figure 1—Acute L-NAME treatment increases BP, reduces capillary diameter, and decreases NO signaling. *A*: Mean arterial pressure (MAP) measured through an indwelling carotid artery catheter in saline-treated (n = 4) and L-NAME–treated (n = 4) mice. Mice were anesthetized with a ketamine/xylazine/acepromazine cocktail (KXA) and treated with either saline or 30 mg/kg L-NAME at $t = -15$ min. At t = 0 min, mice were administered a 4 units/kg insulin bolus (INS), as during the imaging experiments. *B*: MAP values from $t = -10$ min to t = 15 min. *C*: Capillary diameter as a function of time during INS-647 imaging experiments. *D*: Mean diameter of capillaries (rho-dex–labeled vascular structures) at $t = -5$ min. *E* and *F*: Representative immunoblots of phosphorylated VASP (pVASP; S239) (*E*) and total VASP (*F*) and GAPDH in gastrocnemius homogenates. *G–I*: Levels of pVASP (S239) (*G*) and total VASP (*H*) and the ratio of pVASP to VASP (*I*), as determined by densitometric analysis of immunoblots in saline-treated (n = 6) and L-NAME–treated (n = 5) mice. Groups were compared using the Student t test. AU, arbitrary units.

(132.0 mmol/L NaCl, 4.7 mmol/L KCl, 2.0 mmol/L $MgSO_4$, 1.2 mmol/L $CaCl_2$) which was maintained at 37°C and pH 7.4. The exposed gastrocnemius then was imaged using a 20×/0.8 NA Plan-APOCHROMAT air objective on an LSM 780 confocal microscope (Zeiss). To visualize the capillaries of the gastrocnemius, 50 µg of a tetramethylrhodamine-labeled 2-MDa dextran (rho-dex; Thermo Fisher Scientific) vascular marker in 50 µL 0.9% saline was infused into mice through the indwelling jugular vein catheter. After we selected a field of view and acquired a background image, we administered to mice an intravenous bolus of INS-647 (4 units/kg) and 13 µCi 2[^{14}C]deoxyglucose (PerkinElmer). We previously demonstrated that INS-647 is fully bioactive and has the same pharmacodynamics as unlabeled insulin (6). Following the INS-647 bolus, four-slice z-stack images of both the rho-dex and the INS-647 channels were acquired every minute for 15 min. Optical sections were 8 µm in depth (±4 µm about the focal plane) and slices were spaced 4 µm apart to avoid aliasing. After the imaging

experiments, mice were sacrificed and tissues were harvested for analysis.

Image Analysis and Quantification

Images were inspected visually before analysis. Individual frames were removed if we observed major motion artifacts, significant leakage of the vascular marker, or fields of view with very few capillary segments. In total, ~2% of all acquired frames were excluded. After quality control, images were analyzed and quantified as described previously (6). The rho-dex vascular marker channel was used to segment the intravascular and interstitial spaces with the use of an automated Otsu thresholding-based segmentation algorithm. INS-647 intensity was subsequently measured as a function of time in the vascular and interstitial spaces. The interstitial space was defined as the region emanating 1 to 3 μm from the capillary wall. Extravascular INS-647 was measured by using the capillary mask from the vascular segmentation algorithm, dilating the mask 1 μm, and then inverting the mask to measure mean INS-647 intensity in the entire extravascular space.

We used as an index of TIE the ratio of plasma to interstitial INS-647 intensity as a function of time. To quantify the equilibration of plasma INS-647 with the interstitial space, we calculated the exponential decay constant of the first 5 min of the plasma–interstitial INS-647 decay curve by fitting the plasma-to-interstitial ratio data to a monoexponential decay function. We calculated the area under the extravascular INS-647 curve using trapezoidal integration as a measure of total insulin delivery. Baseline (t = 0 min) extravascular insulin values were subtracted from areas under the curve so as to measure the rise in extravascular insulin over the course of the experiment. Mean capillary diameter was estimated with the use of a simplified version of an algorithm developed by McClatchey et al. (37) to measure mitochondrial width. We used the rho-dex vascular marker channel to calculate the ratio of total vascular surface area to total vascular perimeter. This ratio approximates the radius of long, cylindrical vessel segments. Plasma-perfused surface area was calculated by summing the rho-dex surface areas on images of all four slices at a given time point.

Albumin Permeability Imaging

To determine the effects of 4 units/kg insulin on the barrier properties of the capillary endothelium, we performed intravital imaging of BSA labeled with Alexa Fluor 647 (BSA-647). The image acquisition and analysis procedures were the same as those described for INS-647 imaging. Mice were administered a 5 mg/kg bolus of BSA-647 through the indwelling jugular vein catheter (Thermo Fisher Scientific). After acquiring five background images of BSA-647, mice were treated with either 4 units/kg insulin or vehicle (0.1% unlabeled BSA in saline). Images were then acquired every minute for 15 min.

Blood Pressure

BP was measured in a separate cohort of mice undergoing the same treatment protocols for intravital microscopy. Mean arterial pressure was measured through an indwelling carotid artery catheter connected to a transducer and a BPA-400 BP analyzer (Digi-Med). Of note, we observed no difference in BP between control mice receiving a bolus and those receiving continuous infusion of saline. Because of the similar timing of the experiments (a 15-min treatment window), and in an effort to minimize the number of animals used, SNP-treated mice and L-NAME–treated mice were compared with the same control group (50 μL saline bolus).

To assess the ability of SMTC to inhibit nNOS without altering eNOS activity, we measured the BP response to injections of 10 μg/kg acetylcholine (ACh) (33,38). ACh induces rapid and transient hypotension via eNOS-mediated NO production. Thus, a lack of effect of SMTC on the hypotensive response to ACh injection indicates preserved eNOS function. Mice were treated with a bolus of 0.56 μg/kg SMTC or an equivalent volume of saline, and the BP response to three successive ACh injections were measured 15 min later. The three measurements then were averaged to give a single value per mouse.

Insulin Tolerance Tests

Frequently sampled intravenous insulin tolerance tests were performed in conscious, continuously catheterized mice. At t = −15 min, mice received an intravenous bolus of either 30 mg/kg L-NAME or an equivalent volume of saline (50 μL). At t = 0 min, mice received an intravenous bolus of 25 mU/kg insulin (Novolin R; Novo Nordisk) diluted in 0.1% BSA (Sigma-Aldrich) in 0.9% saline. Arterial whole-blood glucose was measured with a Contour blood glucose meter (Bayer) at t = −5, 1, 2, 3, 4, 5, 6, 7, 8, 9, 10, and 15 min.

Measurement of Isotopic Glucose Tracer Accumulation

Accumulation of 2[^{14}C]deoxyglucose-6-phosphate (2[^{14}C]DGP) in gastrocnemius muscle was measured as previously described (16). Because of the difficulty of collecting samples during intravital microscopy for use in measuring 2-deoxy-D-glucose (2DG) in plasma, data are reported as 2DGP accumulation (disintegrations per minute per milligram tissue per minute). Of note, all mice were exposed to the same absolute amount of 2[^{14}C]DG (they all received the same dose of 2[^{14}C]DG), and there was no difference in body weight between groups (data not shown).

Western Blotting

Gastrocnemius homogenates were prepared from tissue collected after intravital microscopy experiments, as described previously (16). Homogenates were separated on 4–12% SDS-PAGE gels (NuPAGE) and transferred to polyvinylidene fluoride membranes. Membranes were blocked with Odyssey Blocking Buffer (LI-COR) and probed with antibodies against total vasodilator-stimulated phosphoprotein (VASP; 1:500; no. 3112; Cell Signaling Technology), phosphorylated (Ser^{239}) VASP (1:500; no. 3114; Cell Signaling Technology), and GAPDH (1:1,000; ab9484; Abcam). Primary antibodies were detected using either

IRDye 800CW goat anti-rabbit (1:5,000; LI-COR) or IRDye 680RD goat anti-mouse (1:10,000; LI-COR) secondary antibodies. Membranes were imaged with an Odyssey Imaging System (LI-COR) and quantified by densitometric analysis with ImageJ software. All Western blotting densitometry data are normalized to the mean of data from the saline-treated control group.

Statistics

All statistical analyses were performed using Prism 7 software (GraphPad Software Inc.). The Grubbs test was performed to detect individual outliers. One statistical outlier was removed from the immunoblot analysis of VASP phosphorylation in the phenylephrine treatment group. Data are presented as the mean ± SEM. Groups were compared either by an unpaired Student *t* test or by one-way ANOVA followed by the Dunnett test to correct for multiple comparisons with a control group (saline treatment).

RESULTS

Acute L-NAME Treatment Accelerates TIE

We first tested the hypothesis that acutely reducing NO would impair insulin transport, as suggested by studies using cultured bovine aortic ECs (23). To reduce endothelial NO levels, we treated mice with L-NAME, an inhibitor of all three NOS isoforms that reduces endothelial NO production (39). Mice received a 30 mg/kg i.v. bolus of L-NAME 15 min before intravital insulin imaging. As expected, treatment of mice with L-NAME increased BP by ~30 mmHg throughout the course of the experiment (Fig. 1*A* and *B*). L-NAME treatment also reduced capillary diameter by ~0.4 μm both before (Fig. 1*C* and *D*) and after (Fig. 1*C*) the insulin bolus. Finally, L-NAME treatment dampened vascular NO signaling as evidenced by lower levels of phosphorylated VASP in the gastrocnemius (Fig. 1*E–I*). These results suggest that L-NAME treatment effectively reduces vascular NO levels.

After confirming that L-NAME reduced NO levels, we imaged insulin in vivo as described in RESEARCH DESIGN AND METHODS. Acute reduction of NO by L-NAME accelerated TIE kinetics by ~30% (Fig. 2). In particular, L-NAME increased the dissipation rate of the plasma–interstitial INS-647 (fluorescent insulin probe) gradient, indicating faster movement of insulin across the endothelium (Fig. 2*B* and *C* and Supplementary Fig. 1*A*). This increase in TIE was not due to changes in the rate of insulin clearance from the plasma, which reflects whole-body insulin clearance (Fig. 2*D*), but rather increased insulin appearance within the SkM interstitial space (Fig. 2*E*). Furthermore, there was no difference in plasma-perfused surface area between saline- and L-NAME–treated mice (Supplementary Fig. 1*B*). Therefore L-NAME, which increased capillary permeability to insulin without altering the surface area available for insulin exchange, enhanced total extravascular insulin delivery (Supplementary Fig. 1*C* and *D*). Thus acute reduction of systemic NO by L-NAME accelerates the movement of insulin across the endothelium and increases total insulin delivery.

To evaluate the possibility that the high dose of INS-647 (4 units/kg) used for intravital microscopy may itself alter endothelial permeability, we performed intravital imaging of BSA-647 (Supplementary Fig. 2*A*). Microvascular permeability to albumin is commonly considered to be an indicator of endothelial barrier function (40), as basal capillary permeability to albumin is very low but can increase under certain inflammatory conditions. We found that the ratio of plasma BSA-647 to interstitial BSA-647 was very stable over time, indicating normal capillary barrier function (Supplementary Fig. 2*B*). It is important to note that treating mice with 4 units/kg insulin had no effect on the ratio of plasma BSA-647 to interstitial BSA-647 (Supplementary Fig. 2*B*). Thus, 4 units/kg insulin does not alter capillary permeability to albumin. These findings confirm that the effect of L-NAME to increase TIE occurs in the setting of normal capillary barrier function.

Acute L-NAME Treatment Enhances the Kinetics of Insulin-Induced Glucose Lowering

After administering the 4 units/kg INS-647 bolus during intravital microscopy experiments, we observed that the blood glucose in L-NAME–treated mice was ~55 mg/dL lower than that in saline-treated mice (Supplementary Fig. 3*A*), reflecting an increase in insulin sensitivity. Furthermore, L-NAME treatment resulted in a nonsignificant 35% increase in the accumulation of the isotopic glucose tracer 2[^{14}C]DGP (Supplementary Fig. 3*B*). These results suggest that acute L-NAME treatment enhances insulin-stimulated glucose metabolism.

To more comprehensively assess the effects of L-NAME on insulin sensitivity, we performed frequently sampled intravenous insulin tolerance tests (Fig. 3). We chose to perform insulin tolerance tests in order to mimic the experimental design of the intravital microscopy experiments, which also assessed responses to an insulin bolus. After treatment with a 25 mU/kg insulin bolus, L-NAME-treated mice displayed a more rapid reduction in glucose than did saline-treated mice (Fig. 3*A* and *B*). Namely, L-NAME treatment increased the fractional reduction in glucose per minute by ~40% (Fig. 3*C*). These findings demonstrate that acute L-NAME treatment accelerates glucose lowering following an intravenous insulin bolus.

nNOS Inhibition Does Not Affect TIE Kinetics

L-NAME inhibits all three NOS isoforms. The expression and activity of inducible NOS (iNOS) in SkM are minimal during basal, noninflammatory conditions (41), such as those used in our intravital microscopy experiments (6). Thus the effects of L-NAME are most likely mediated by one of the constitutive NOS isoforms, eNOS or nNOS, both of which are expressed in ECs and contribute to vascular function.

To determine whether nNOS contributes to the effects of L-NAME on TIE, we treated mice with SMTC (0.56 μg/kg),

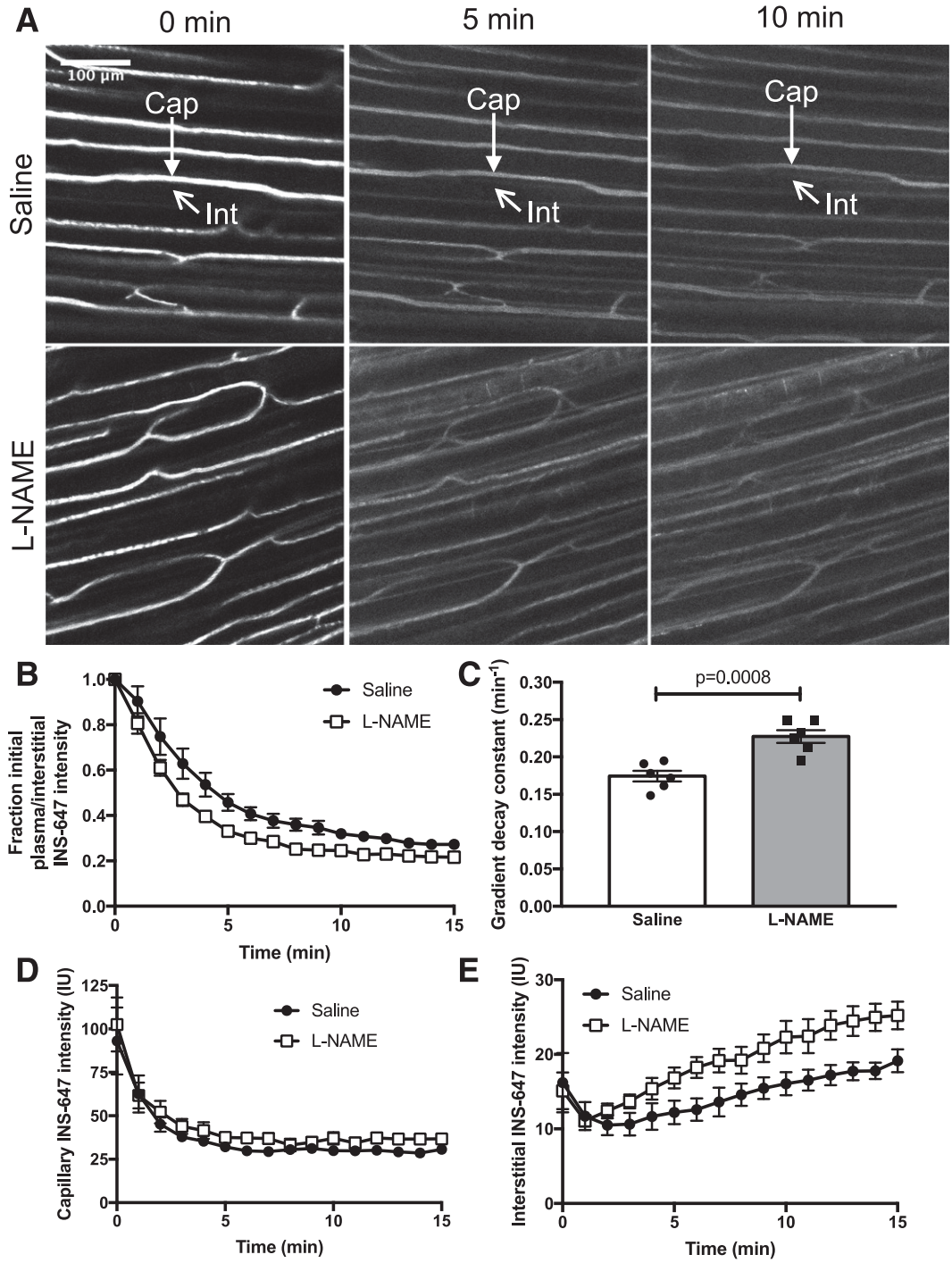

Figure 2—Acute inhibition of NOS by L-NAME enhances TIE. *A*: Representative INS-647 images (maximal intensity projections) from mice treated with either saline ($n = 6$) or L-NAME (30 mg/kg i.v.; $n = 6$) 15 min before administration of the 4 units/kg INS-647 bolus. Block arrows indicate the capillaries (Cap) and skeleton arrows, the interstitial space (Int). *B*: The ratio of plasma INS-647 to interstitial INS-647 as a function of time after injection of INS-647 normalized to the ratio at $t = 0$ min. *C*: The exponential decay constant of the plasma-to-interstitial INS-647 ratio, a measure of insulin efflux kinetics. *D* and *E*: Capillary (*D*) and interstitial (*E*) INS-647 intensities as functions of time after INS-647 injection. Interstitial INS-647 intensity is defined as the mean INS-647 intensity between 1 and 3 μm from the capillary wall. Groups were compared using the Student *t* test. IU, intensity units.

a NOS inhibitor with 17-fold greater selectivity for nNOS over eNOS (31). SMTC treatment reduced plasma-perfused surface area by 33% (Supplementary Fig. 4*A* and *B*). While the effect of SMTC on capillary perfusion was not statistically significant, the magnitude of the effect is similar to the magnitude of reductions caused by SMTC in resting blood flow and vascular conductance reported previously (~25–40%) (32,42). SMTC treatment did not

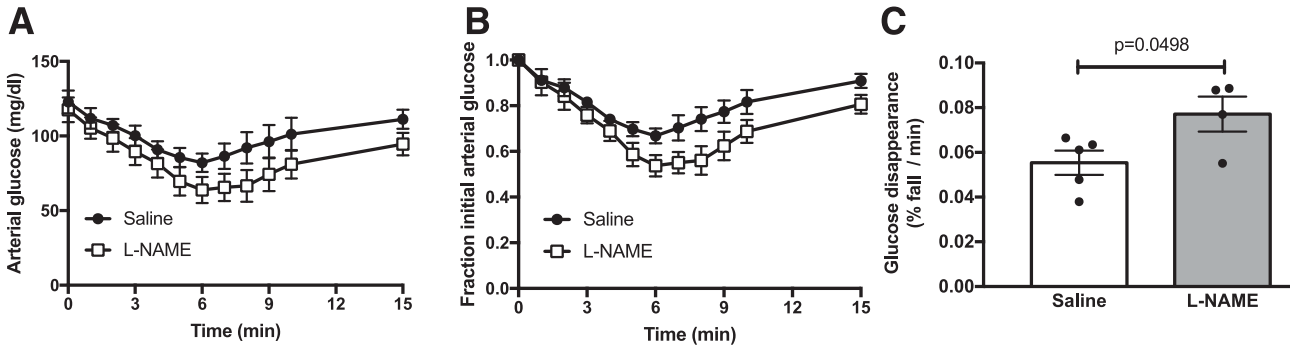

Figure 3—Acute L-NAME treatment accelerates insulin-induced glucose lowering in conscious, unstressed mice. *A*: Arterial glucose excursions after a 25 mU/kg insulin bolus (t = 0 min) in mice treated with saline (n = 5) or L-NAME (n = 4) 15 min before the insulin bolus. *B*: Glucose excursions from *A* displayed as a fraction of arterial glucose levels at t = 0 min. *C*: Rate of disappearance of fractional glucose from t = 0 to t = 6 min; this is an index of insulin sensitivity.

change capillary diameter (Supplementary Fig. 4*C*). Furthermore, SMTC had no effect on the hypotensive response to ACh (Supplementary Fig. 4*D*). These findings suggest that SMTC selectively inhibits nNOS without altering eNOS function.

nNOS inhibition had no effect on the movement of insulin across the endothelium (Fig. 4). Specifically, SMTC did not alter the rate at which INS-647 equilibrated with the interstitial space (Fig. 4*B* and *C* and Supplementary Fig. 5*A*), nor did it change the plasma or interstitial kinetics of INS-647 (Fig. 4*D* and *E*). Furthermore, we did not observe any effect of SMTC on the total extravascular delivery of insulin (Supplementary Fig. 5*B* and *C*). Consistent with these findings, SMTC treatment did not affect the accumulation of 2[^{14}C]DGP in the gastrocnemius after the imaging experiment (Supplementary Fig. 5*D*). These results collectively indicate that nNOS inhibition does not alter TIE. Given that iNOS activity is minimal under basal conditions and that nNOS inhibition has no effect on TIE, we can infer that eNOS inhibition mediates the effects of L-NAME on TIE.

Acute NO Donor Treatment Does Not Affect TIE Kinetics

In light of the finding that reducing endothelial NO with L-NAME enhanced TIE, we hypothesized that acutely increasing the amount of NO would have the opposite effect. To test this hypothesis, we treated mice with a 100 μg/kg/min continuous infusion of SNP, an NO donor. SNP reduced mean BP by 10 mmHg during the treatment period before insulin stimulation (Supplementary Fig. 6*A* and *B*). Insulin abolished the hypotensive effect of SNP (Supplementary Fig. 6*A* and *B*). Capillary diameter was unaffected by SNP (Supplementary Fig. 6*C* and *D*). Finally, the ratio of phosphorylated to total VASP, an index of vascular NO signaling, was increased by ∼40%, although this difference was not significant (Supplementary Fig. 6*E–I*). These findings indicate that SNP modestly elevates NO levels.

Using intravital insulin imaging, we observed that SNP had no effect on TIE kinetics (Fig. 5). In particular, SNP altered neither the dissipation rate of the plasma–interstitial INS-647 gradient (Fig. 5*B* and *C* and Supplementary Fig. 7*A*) nor INS-647 kinetics in plasma and the interstitial space (Fig. 5*D* and *E*). Furthermore, as SNP had no effect on plasma-perfused surface area (Supplementary Fig. 7*B*), it did not change total extravascular insulin delivery (Supplementary Fig. 7*C* and *D*). Consistent with the lack of an effect of SNP on TIE kinetics and insulin delivery, SNP altered neither blood glucose (Supplementary Fig. 8*A*) nor the accumulation of 2[^{14}C]DGP in the gastrocnemius after the imaging experiment (Supplementary Fig. 8*B*). These findings suggest that acutely increasing NO with SNP in otherwise healthy mice has no effect on TIE.

Neither a Direct Smooth Muscle–Acting Constrictor nor a Dilator Affects TIE Kinetics

As described above, L-NAME treatment accelerates TIE kinetics and increases BP. To test whether the effects of L-NAME on TIE kinetics are solely due to changes in BP, we modulated BP with drugs that act directly on smooth muscle—namely, phenylephrine, which raises BP, and hydralazine, which lowers BP (28,29). Compared with saline-treated mice, phenylephrine raised BP by ∼15 mmHg, whereas hydralazine lowered it by the same amount (Supplementary Fig. 9*A* and *B*). Phenylephrine treatment reduced the initial capillary diameter by ∼0.6 μm (Supplementary Fig. 9*C* and *D*), although this effect was not sustained after the insulin bolus was administered (Supplementary Fig. 9*C*). Hydralazine had no effect on capillary diameter (Supplementary Fig. 9*C* and *D*). It is interesting to note that phenylephrine increased the phosphorylation of VASP relative to that in saline-treated mice (Supplementary Fig. 9*E–I*). Hydralazine treatment did not alter VASP phosphorylation (Supplementary Fig. 9*E–I*).

Intravital imaging of insulin efflux revealed that neither phenylephrine nor hydralazine affected the rate at which insulin transited the endothelium (Fig. 6*B* and *C* and

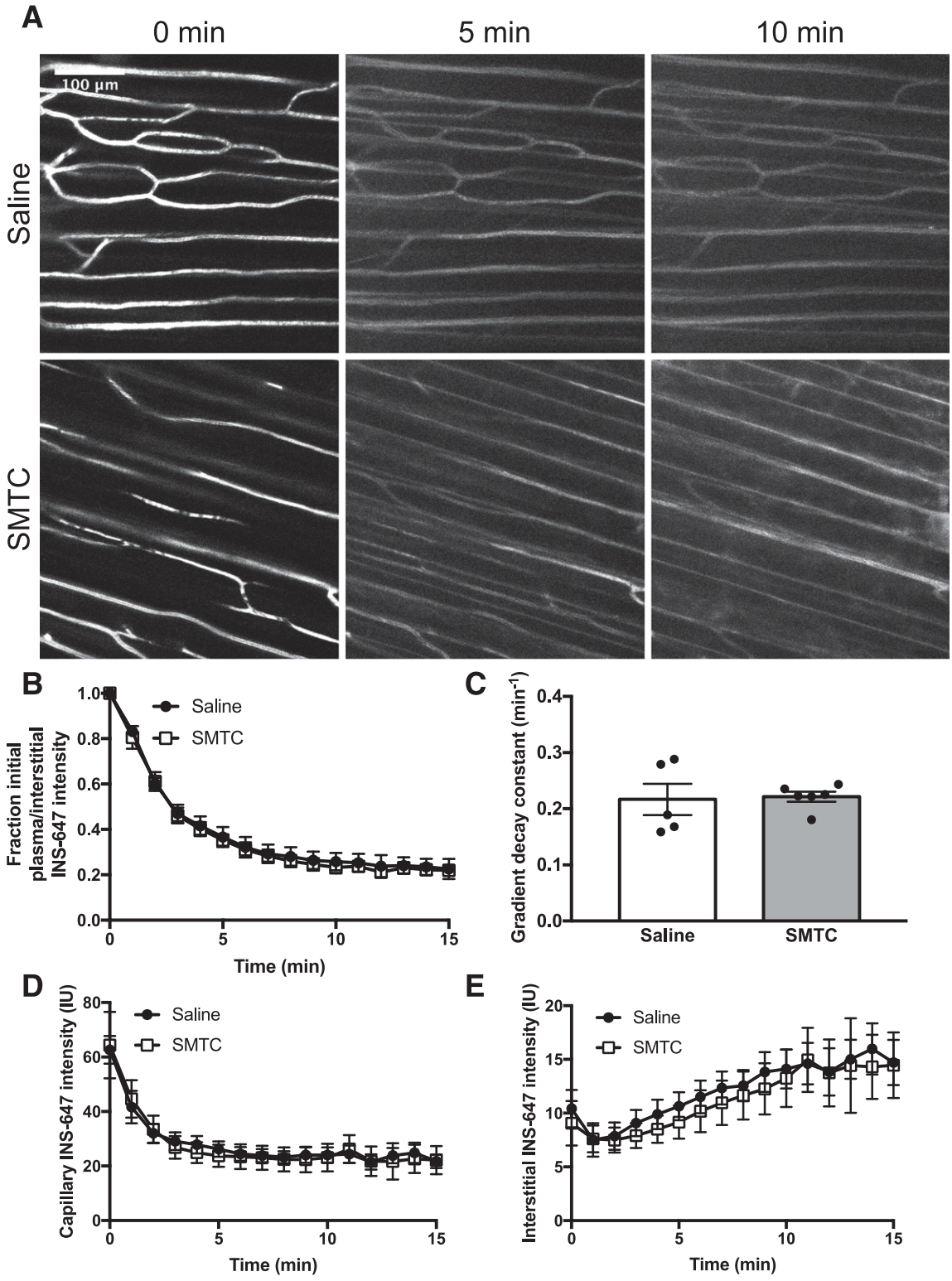

Figure 4—Selective nNOS inhibition does not affect TIE. *A*: Representative INS-647 images (maximal intensity projections) from mice treated with either saline (n = 5) or SMTC (0.56 mg/kg i.v.; n = 6) 5 min before administration of the 4 units/kg INS-647 bolus. *B*: The ratio of plasma INS-647 to interstitial INS-647 as a function of time after injection of INS-647 normalized to the ratio at t = 0 min. *C*: The exponential decay constant of the plasma-to-interstitial INS-647 ratio, a measure of insulin efflux kinetics. *D* and *E*: Capillary (*D*) and interstitial (*E*) INS-647 intensities as functions of time after INS-647 injection. Interstitial INS-647 intensity is defined as the mean INS-647 intensity between 1 and 3 μm from the capillary wall. Groups were compared using the Student t test. IU, intensity units.

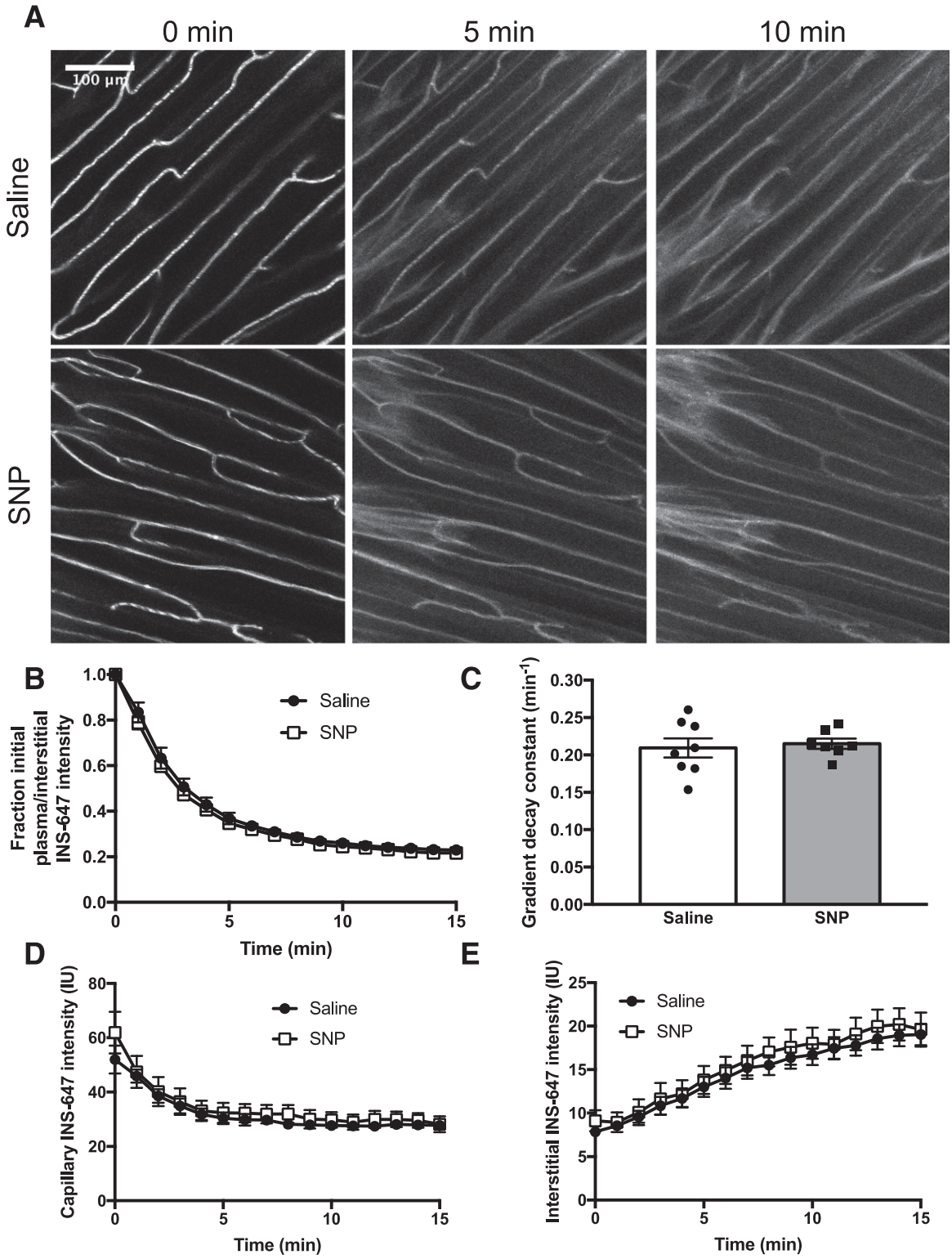

Figure 5—SNP, an NO donor, has no effect on TIE kinetics. *A*: Representative INS-647 images (maximal intensity projections) from mice treated with either saline (n = 8) or 100 μg/kg/min SNP (n = 7). Continuous infusions of saline or SNP were begun 15 min before the INS-647 bolus was administered and continued throughout the experiment. *B*: The ratio of plasma INS-647 to interstitial INS-647 as a function of time after injection of INS-647 normalized to the ratio at t = 0 min. *C*: The exponential decay constant of the plasma-to-interstitial INS-647 ratio, a measure of insulin efflux kinetics. *D* and *E*: Capillary (*D*) and interstitial (*E*) INS-647 intensities as functions of time after INS-647 injection. Interstitial INS-647 intensity is defined as the mean INS-647 intensity between 1 and 3 μm from the capillary wall. Groups were compared using the Student t test. IU, intensity units.

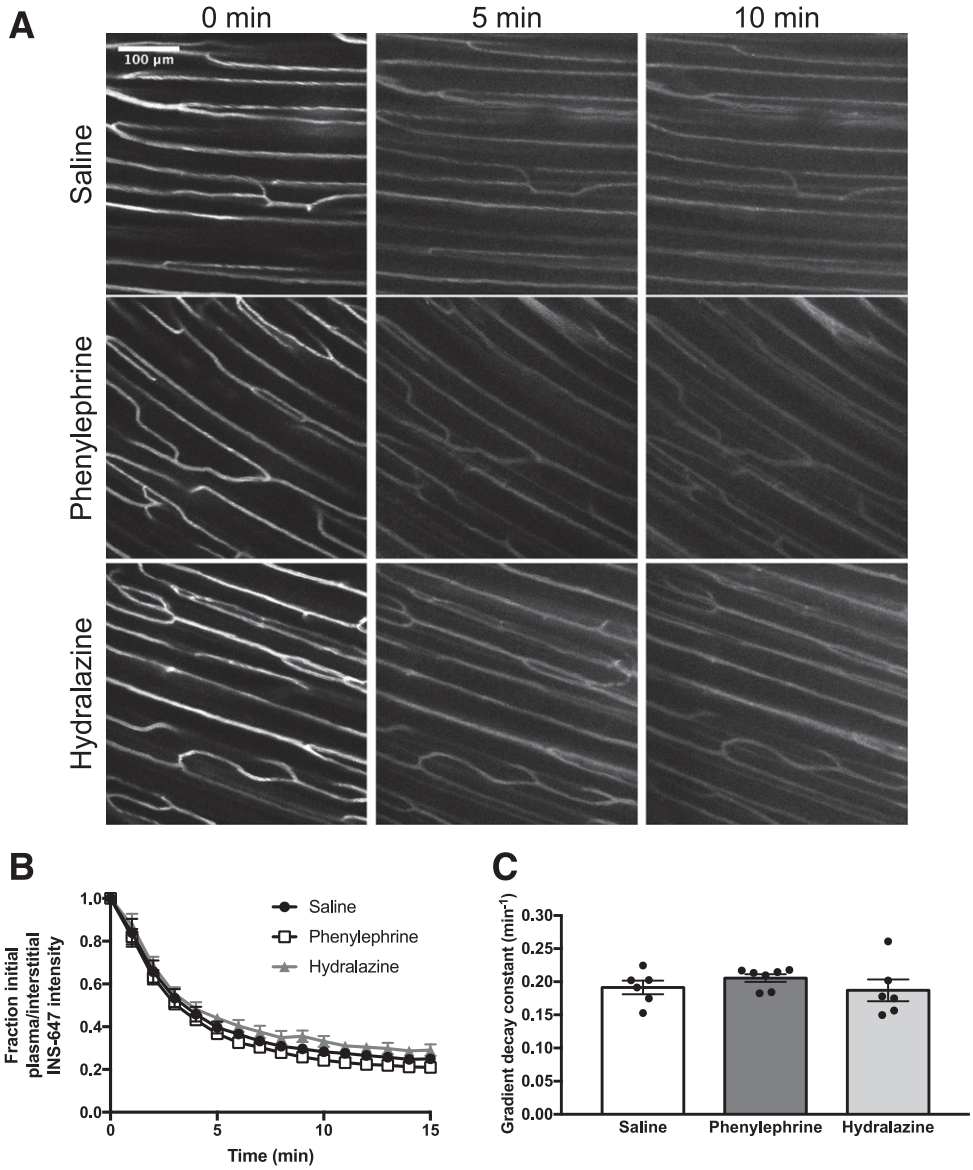

Figure 6— Neither a vasoconstrictor nor a dilator that acts directly on smooth muscle alters TIE. *A*: Representative INS-647 images (maximal intensity projections) from mice treated with saline ($n = 6$), phenylephrine ($n = 7$), or hydralazine ($n = 6$). Primed, continuous infusions of saline, phenylephrine (300 μg/kg bolus, 300 μg/kg/min continuous infusion), or hydralazine (1 mg/kg bolus, 1 mg/kg/min continuous infusion) were begun 5 min before the INS-647 bolus was administered. *B*: The ratio of plasma INS-647 to interstitial INS-647 as a function of time after injection of INS-647 normalized to the ratio at $t = 0$ min. *C*: The exponential decay constant of the plasma-to-interstitial INS-647 ratio, a measure of insulin efflux kinetics. Groups were compared using one-way ANOVA followed by the Dunnett test for multiple comparisons to a control (saline-treated) group.

Supplementary Fig. 10). Of note, phenylephrine did seem to enhance the clearance of INS-647 from the plasma, but this was also associated with a reduced amount of INS-647 in the interstitial space in SkM (Supplementary Fig. 11*A*–*D*). This suggests that, while phenylephrine may enhance the whole-body clearance of insulin from the plasma by other organs (Supplementary Fig. 11*B*), it did not change TIE in SkM capillaries (Fig. 6*C*). Phenylephrine had no effect on plasma-perfused surface area (Supplementary Fig. 11*E*); therefore, combined with its effect to dampen interstitial INS-647 appearance (Supplementary Fig. 11*C*), it also reduced total extravascular insulin delivery (Supplementary Fig. 11*F* and *G*). Thus, it seems that while phenylephrine does not affect either TIE or the surface area available for insulin exchange, it diverts insulin away from SkM by increasing its clearance by other organs. These findings indicate that increasing or decreasing BP by ~15 mmHg with the use of drugs that act directly on smooth muscle does not affect TIE.

With respect to glucose metabolism, phenylephrine resulted in a nonsignificant ~50 mg/dL increase in glucose after intravital insulin imaging (Supplementary Fig. 12*A*). Furthermore, phenylephrine reduced the accumulation of 2[^{14}*C*]DGP in the gastrocnemius, indicating that it induces

insulin resistance in SkM (Supplementary Fig. 12*B*). Hydralazine had no effect on either blood glucose or gastrocnemius 2[^{14}C]DGP accumulation (Supplementary Fig. 12*B*). These results suggest that phenylephrine induces insulin resistance in SkM through a mechanism that does not involve alterations to TIE kinetics.

DISCUSSION

In this study we used intravital imaging of fluorescently labeled insulin to show that acute reduction of endothelial NO with L-NAME accelerates the rate at which insulin moves across the endothelium in SkM capillaries. While L-NAME reduced capillary diameter, it also increased the total amount of insulin delivered to the muscle. This indicates that, with respect to insulin delivery, increases in TIE outweigh any decreases in perfusion caused by L-NAME. These increases in TIE kinetics and insulin delivery were associated with accelerated whole-body insulin action. It is interesting that treatment with SNP, an NO donor, did not alter TIE kinetics. Furthermore, phenylephrine, a vasoconstrictor that acts directly on smooth muscle, had no effect on TIE kinetics, indicating that the effects of L-NAME on TIE kinetics are not solely due to BP changes. These findings demonstrate that acute pharmacological NO reduction induces changes to the SkM microvasculature that increase insulin efflux and delivery.

Several previous studies have investigated the effects of NO on microvascular permeability. With respect to insulin, Wang et al. (23) demonstrated that inhibition of NO by L-NAME reduced the uptake of fluorescein isothiocyanate–labeled insulin into cultured bovine aortic ECs. This finding suggests that NO is a positive regulator of TIE in vitro, which is seemingly at odds with the results of the current study showing that L-NAME enhances TIE in vivo. It is conceivable that L-NAME may block the nonspecific vesicular uptake of insulin into ECs and thereby promote more efficient paracellular movement of insulin through interendothelial junctions. In addition, the hemodynamic effects of L-NAME on the microvasculature, which occur in vivo but not in vitro, may contribute to the contrasting results. Another important consideration is that the mechanism of TIE is different in vivo than in cell culture and depends on the type of ECs used (43). With our intravital microscopy technique, we can directly visualize and quantitate the movement of insulin across the endothelium of SkM capillaries in vivo.

Other groups have assessed the effects of NO modulation in vivo on microvascular permeability to macromolecules besides insulin. While the precise effects of NO on capillary permeability are still debated, it is clear that they are dependent on context (26,44). Under basal conditions, NO reduction by NOS inhibition increases capillary permeability in a number of different species and vascular beds, including SkM (45–47). On the other hand, hyperproduction of NO during pathological inflammatory states also seems to increase capillary permeability (44). Thus the relation between endothelial NO production and microvascular permeability seems to be U-shaped, with low and high levels of NO being associated with increased capillary permeability. This is consistent with the current study, which showed that reduction of NO with L-NAME in a noninflammatory state increases the permeability of SkM capillaries to insulin. It is interesting that increasing NO availability in otherwise healthy mice with SNP had no effect on capillary permeability to insulin. It is possible that high levels of NO increase microvascular permeability only during inflammatory conditions in which oxidant production is also elevated.

Our findings suggest that, at the molecular level, the effect of L-NAME is mediated by eNOS inhibition because nNOS inhibition had no effect on TIE, and because eNOS knockout mice, but not iNOS knockout mice, display enhanced SkM vascular permeability (47). One caveat is that the reduction in plasma-perfused surface area caused by SMTC, while similar in magnitude to previously reported effects of SMTC on SkM blood flow (32,42), was not statistically significant. Because of this, we cannot rule out a minor contribution of nNOS inhibition to the effects of L-NAME.

Mechanistically, the effect of L-NAME on TIE was not due to changes in BP alone; phenylephrine also raised BP but did not alter TIE. These findings suggest that L-NAME increases TIE either through direct effects on the capillary endothelium or by altering the transcapillary balance of Starling forces. Our previous work demonstrated that insulin moves across the capillary endothelium in SkM either through a convective paracellular route or through nonsaturable vesicular transcytosis (6). Malik and colleagues (47) used electron microscopy to show that treatment with L-NAME opens interendothelial junctions in mice. This increased distance between ECs would allow for enhanced paracellular extravasation of insulin across the endothelium, consistent with our previous findings. The mechanism by which L-NAME widens interendothelial junctions may involve alterations in junction protein nitrosylation or increased leukocyte/platelet-endothelial interactions. In fact, Kurose et al. (45) demonstrated that the L-NAME-induced increase in albumin extravasation from mesenteric venules could be attenuated by using monoclonal antibodies that block adherence of leukocytes and platelets to the endothelium. In addition to potential biochemical and cellular effects, L-NAME reduced capillary diameter, indicating that L-NAME treatment most likely alters capillary hemodynamics. These hemodynamic effects may alter the balance of Starling forces across the endothelium and subsequently the convective movement of insulin into the interstitial space. Finally, it is also conceivable that reduction of endothelial NO production affects the abundance of endothelial vesicles and pores.

Consistent with the increases in TIE and insulin delivery, we found that acute inhibition of NOS with L-NAME increased the effect of insulin on whole-body glucose kinetics. This corroborates the findings of Vincent et al. (20),

who showed that after 15 min of continuous infusion of insulin and L-NAME in rats, L-NAME increased femoral artery blood flow without changing the hindlimb arteriovenous glucose difference. This indicates that L-NAME enhances insulin-stimulated glucose uptake in muscle at this early time point. Interestingly, Vincent et al. also showed that the hindlimb arteriovenous glucose difference was reduced by t = 30 min, whereas femoral artery blood flow remained elevated in the L-NAME-treated group, indicating a small reduction in insulin-stimulated glucose uptake in muscle. These findings suggest that L-NAME initially increases insulin action in SkM, whereas more prolonged administration results in insulin resistance in SkM.

Previous studies in humans and rodents have generally found a negative relation between NOS inhibition and SkM insulin sensitivity during hyperinsulinemic-euglycemic clamps (17–19). In the current study we showed that L-NAME accelerated insulin-stimulated glucose lowering during an insulin tolerance test. Differences in study design may explain these seemingly contradictory findings. Hyperinsulinemic-euglycemic clamps, as used previously (17–19), are usually designed to assess steady-state insulin action, whereas the response of glucose to an insulin bolus is an indicator of the kinetics of insulin action. Thus it is possible that L-NAME treatment enhances the kinetics of insulin-stimulated glucose disposal while also reducing maximal, steady-state insulin-stimulated glucose disposal. These differing effects can be reconciled if one considers that L-NAME both increases the movement of insulin across the endothelium and reduces SkM perfusion (17,20). We hypothesized that the effect of L-NAME to increase capillary permeability to insulin accelerates the kinetics of insulin action. On the other hand, the L-NAME-induced reduction in SkM perfusion is most likely responsible for limiting maximal steady-state insulin-stimulated glucose uptake in muscle.

A key distinction between the present work and studies using genetic deletion of eNOS (21,22) is the amount of time for which NO levels are reduced. eNOS knockout mice experience a chronic attenuation of NO levels, which is different than the acute inhibition of NO production by L-NAME. eNOS knockout mice display peripheral insulin resistance during hyperinsulinemic-euglycemic clamps (21,22), whereas acute L-NAME treatment accelerates the glucose-lowering effects of an insulin bolus. These differences may be explained by adaptations of SkM to the long-term reduction of NO in eNOS knockout mice. For instance, mitochondrial dysfunction, excessive lipid accumulation, and arteriolar rarefaction have all been observed in eNOS knockout mice (48,49). Each of these pathological processes would be expected to contribute to the insulin resistance in SkM observed in eNOS knockout mice. In contrast to chronic NO reduction, acute L-NAME treatment would not be able to induce these changes during the short time frame of the experiment. Instead, acute NOS inhibition enhances the delivery of an insulin bolus to SkM by increasing the rate at which insulin moves across the endothelium.

In light of the finding that L-NAME increases TIE kinetics, we hypothesized that treating mice with SNP, an NO donor, would have the opposite effect. However, we found that NO had no effect on either TIE or accumulation of 2[^{14}C]DGP in the gastrocnemius. This finding is largely consistent with those of previous studies, which showed that SNP infusion either does not alter insulin-stimulated glucose disposal (50) or slightly reduces it (34). One limitation of our study is that, despite infusing a high dose of SNP, which was previously shown to have major cardiovascular and metabolic effects (34), BP was lowered by only ~10 mmHg, and the 40% increase in VASP activation (i.e., NO signaling) was not significant. The BP response to SNP may have been attenuated because mice were already hypotensive when anesthetized. Furthermore, because insulin stimulates NO production by ECs (51), it is possible that NO signaling is already near maximum in the saline-treated control mice. In this situation, SNP may have little additional effect on VASP activation. As such, we hypothesize that, under conditions where endothelial NO is sufficient, adding more NO gives no further benefit to TIE kinetics or to SkM insulin sensitivity.

As noted above, we also demonstrated that while phenylephrine and hydralazine raise and lower BP, respectively, neither drug altered TIE. These findings suggest that the L-NAME-induced increase in TIE is not due to elevated BP alone. One caveat, however, is that L-NAME raised BP by 30 mmHg, whereas phenylephrine raised it by only 15 mmHg. Thus it is possible that a more pronounced increase in BP might affect TIE. In contrast to the effect of L-NAME, phenylephrine induced insulin resistance in SkM during intravital microscopy experiments, although this was not due to a change in TIE. It is possible that phenylephrine induced insulin resistance in SkM either by diverting insulin to other organs or by limiting the microvascular delivery of glucose to SkM. Interestingly, we observed increased VASP phosphorylation at Ser^{239} in the gastrocnemius of mice treated with phenylephrine. It is unclear whether this effect is due to increased NO production per se or to signaling through a different serine-threonine kinase pathway (52). Regardless of the mechanism of phenylephrine-stimulated VASP Ser^{239} phosphorylation, increasing BP without reducing NO does not change TIE.

Our study has some limitations that should be considered. First, we administered L-NAME into the systemic circulation, where it eventually interacts with a variety of cell types. We attempted to limit the effects of L-NAME on the endothelium by using a short 15-min treatment window. However, it is possible that non-ECs such as smooth muscle cells, pericytes, myocytes, or circulating blood cells may contribute to the effects of L-NAME on TIE and insulin sensitivity within this time frame. It should be noted that L-NAME has no effect on insulin-stimulated glucose uptake in isolated muscles (18,53–55).

This suggests that the increase in insulin sensitivity caused by L-NAME is not due to off-target effects of L-NAME on myocytes. Another limitation to this study is the high dose of INS-647 (4 units/kg) necessary because of the low circulating insulin concentrations and the limited sensitivity of fluorescence intravital microscopy. As shown with BSA-647 imaging, this dose of insulin does not seem to perturb normal capillary barrier function. Furthermore, L-NAME enhanced insulin sensitivity when both high (4 units/kg; intravital microscopy) and low (25 mU/kg; insulin tolerance tests in conscious mice) doses of insulin were administered. Thus the effects of L-NAME seem to be independent of the insulin dose. Finally, it is important to note that VASP is expressed not only in ECs but also in other cell types such as platelets. Thus it is possible that a fraction of the reduced phosphorylated VASP signal measured in SkM homogenates from L-NAME–treated mice emanates from non-ECs. However, we also showed that L-NAME treatment increased BP and reduced capillary diameter. These are hallmarks of NOS inhibition in the endothelium. Taken together, these three pieces of data strongly support the notion that L-NAME reduces endothelial NO production.

In summary, we report the novel observation that reduction of endothelial NO enhances TIE in SkM capillaries in vivo through an eNOS-dependent mechanism. Thus acute reduction of NO levels has contrasting effects on microvascular perfusion and the capillary exchange of insulin, the net effect of which is to increase insulin delivery to SkM. To the best of our knowledge, this is the first report of a pharmacological intervention that increases transendothelial insulin transport and insulin delivery to SkM. The increase in insulin delivery to SkM caused by NOS inhibition was also associated with accelerated insulin action. Our study highlights the functional importance of transendothelial insulin transport and insulin delivery to insulin action in SkM.

Acknowledgments. The authors thank Freyja James and Carlo Malabanan (Department of Molecular Physiology and Biophysics, Vanderbilt University) for performing catheterization surgeries and for assisting with blood pressure measurements. The authors gratefully acknowledge the use of services provided by the Vanderbilt University Cell Imaging Shared Resource, Mouse Metabolic Phenotyping Center, and Diabetes Research and Training Center. Eli Lilly provided the fluorescent insulin probe.

Funding. This work was supported by the National Institute of Diabetes and Digestive and Kidney Diseases (grant nos. F31DK109594 and T32DK007563 to I.M.W. and grant nos. R01DK054902, R37DK050277, and U24DK059637 to D.H.W.)

Duality of Interest. F.A.V. was an employee and shareholder of Eli Lilly and Co. during this study. No other potential conflicts of interest relevant to this article were reported.

Author Contributions. I.M.W. wrote the manuscript. I.M.W. and D.H.W. conceived and designed the study. I.M.W., D.P.B., and F.A.V. performed the experiments and collected data. P.M.M., F.A.V., and D.H.W. edited the manuscript and contributed to the discussion. I.M.W. is the guarantor of this work and, as such, had full access to all the data in the study and takes responsibility for the integrity of the data and the accuracy of the data analysis.

Prior Presentation. Parts of this study were presented at the American Physiological Society Experimental Biology meeting, San Diego, CA, 21–25 April 2018.

References

1. Baron AD. Hemodynamic actions of insulin. Am J Physiol 1994;267:E187–E202
2. Barrett EJ, Wang H, Upchurch CT, Liu Z. Insulin regulates its own delivery to skeletal muscle by feed-forward actions on the vasculature. Am J Physiol Endocrinol Metab 2011;301:E252–E263
3. Clark MG. Impaired microvascular perfusion: a consequence of vascular dysfunction and a potential cause of insulin resistance in muscle. Am J Physiol Endocrinol Metab 2008;295:E732–E750
4. Kolka CM, Bergman RN. The barrier within: endothelial transport of hormones. Physiology (Bethesda) 2012;27:237–247
5. Lee WL, Klip A. Endothelial transcytosis of insulin: does it contribute to insulin resistance? Physiology (Bethesda) 2016;31:336–345
6. Williams IM, Valenzuela FA, Kahl SD, et al. Insulin exits skeletal muscle capillaries by fluid-phase transport. J Clin Invest 2018;128:699–714
7. Yang YJ, Hope ID, Ader M, Bergman RN. Insulin transport across capillaries is rate limiting for insulin action in dogs. J Clin Invest 1989;84:1620–1628
8. Chiu JD, Richey JM, Harrison LN, et al. Direct administration of insulin into skeletal muscle reveals that the transport of insulin across the capillary endothelium limits the time course of insulin to activate glucose disposal. Diabetes 2008;57:828–835
9. Förstermann U, Sessa WC. Nitric oxide synthases: regulation and function. Eur Heart J 2012;33:829–837, 837a–837d
10. Lima B, Forrester MT, Hess DT, Stamler JS. S-nitrosylation in cardiovascular signaling. Circ Res 2010;106:633–646
11. Vanhoutte PM, Shimokawa H, Feletou M, Tang EH. Endothelial dysfunction and vascular disease - a 30th anniversary update. Acta Physiol (Oxf) 2017;219:22–96
12. Sansbury BE, Hill BG. Regulation of obesity and insulin resistance by nitric oxide. Free Radic Biol Med 2014;73:383–399
13. Steinberg HO, Chaker H, Leaming R, Johnson A, Brechtel G, Baron AD. Obesity/insulin resistance is associated with endothelial dysfunction. Implications for the syndrome of insulin resistance. J Clin Invest 1996;97:2601–2610
14. Kubota T, Kubota N, Kumagai H, et al. Impaired insulin signaling in endothelial cells reduces insulin-induced glucose uptake by skeletal muscle. Cell Metab 2011;13:294–307
15. Abuissa H, Jones PG, Marso SP, O'Keefe JH Jr. Angiotensin-converting enzyme inhibitors or angiotensin receptor blockers for prevention of type 2 diabetes: a meta-analysis of randomized clinical trials. J Am Coll Cardiol 2005;46:821–826
16. Williams IM, Otero YF, Bracy DP, Wasserman DH, Biaggioni I, Arnold AC. Chronic angiotensin-(1-7) improves insulin sensitivity in high-fat fed mice independent of blood pressure. Hypertension 2016;67:983–991
17. Baron AD, Steinberg HO, Chaker H, Leaming R, Johnson A, Brechtel G. Insulin-mediated skeletal muscle vasodilation contributes to both insulin sensitivity and responsiveness in lean humans. J Clin Invest 1995;96:786–792
18. Roy D, Perreault M, Marette A. Insulin stimulation of glucose uptake in skeletal muscles and adipose tissues in vivo is NO dependent. Am J Physiol 1998;274:E692–E699
19. Vincent MA, Barrett EJ, Lindner JR, Clark MG, Rattigan S. Inhibiting NOS blocks microvascular recruitment and blunts muscle glucose uptake in response to insulin. Am J Physiol Endocrinol Metab 2003;285:E123–E129
20. Vincent MA, Clerk LH, Lindner JR, et al. Microvascular recruitment is an early insulin effect that regulates skeletal muscle glucose uptake in vivo. Diabetes 2004;53:1418–1423
21. Shankar RR, Wu Y, Shen HQ, Zhu JS, Baron AD. Mice with gene disruption of both endothelial and neuronal nitric oxide synthase exhibit insulin resistance. Diabetes 2000;49:684–687

22. Duplain H, Burcelin R, Sartori C, et al. Insulin resistance, hyperlipidemia, and hypertension in mice lacking endothelial nitric oxide synthase. Circulation 2001; 104:342–345
23. Wang H, Wang AX, Aylor K, Barrett EJ. Nitric oxide directly promotes vascular endothelial insulin transport. Diabetes 2013;62:4030–4042
24. King GL, Johnson SM. Receptor-mediated transport of insulin across endothelial cells. Science 1985;227:1583–1586
25. Jaldin-Fincati JR, Pereira RVS, Bilan PJ, Klip A. Insulin uptake and action in microvascular endothelial cells of lymphatic and blood origin. Am J Physiol Endocrinol Metab 2018;315:E204–207
26. Kvietys PR, Granger DN. Role of reactive oxygen and nitrogen species in the vascular responses to inflammation. Free Radic Biol Med 2012;52: 556–592
27. Ayala JE, Bracy DP, Malabanan C, et al. Hyperinsulinemic-euglycemic clamps in conscious, unrestrained mice. J Vis Exp 2011;(57). pii:3188
28. Jackson WF, Boerman EM, Lange EJ, Lundback SS, Cohen KD. Smooth muscle alpha1D-adrenoceptors mediate phenylephrine-induced vasoconstriction and increases in endothelial cell Ca2+ in hamster cremaster arterioles. Br J Pharmacol 2008;155:514–524
29. Gurney AM, Allam M. Inhibition of calcium release from the sarcoplasmic reticulum of rabbit aorta by hydralazine. Br J Pharmacol 1995;114: 238–244
30. Bursztyn M, Raz I, Mekler J, Ben-Ishay D. Effect of acute N-nitro-L-arginine methyl ester (L-NAME) hypertension on glucose tolerance, insulin levels, and [^{3}H]-deoxyglucose muscle uptake. Am J Hypertens 1997;10:683–686
31. Furfine ES, Harmon MF, Paith JE, et al. Potent and selective inhibition of human nitric oxide synthases. Selective inhibition of neuronal nitric oxide synthase by S-methyl-L-thiocitrulline and S-ethyl-L-thiocitrulline. J Biol Chem 1994;269: 26677–26683
32. Wakefield ID, March JE, Kemp PA, Valentin J-P, Bennett T, Gardiner SM. Comparative regional haemodynamic effects of the nitric oxide synthase inhibitors, S-methyl-L-thiocitrulline and L-NAME, in conscious rats. Br J Pharmacol 2003; 139:1235–1243
33. Hirai DM, Copp SW, Ferguson SK, et al. Neuronal nitric oxide synthase regulation of skeletal muscle functional hyperemia: exercise training and moderate compensated heart failure. Nitric Oxide 2018;74:1–9
34. House LM 2nd, Morris RT, Barnes TM, et al. Tissue inflammation and nitric oxide-mediated alterations in cardiovascular function are major determinants of endotoxin-induced insulin resistance. Cardiovasc Diabetol 2015; 14:56
35. Boesen EI, Pollock DM. Effect of chronic IL-6 infusion on acute pressor responses to vasoconstrictors in mice. Am J Physiol Heart Circ Physiol 2007;293: H1745–H1749
36. Robinson MA, Welsh DC, Bickel DJ, Lynch JJ, Lyle EA. Differential effects of sodium nitroprusside and hydralazine in a rat model of topical FeCl3-induced carotid artery thrombosis. Thromb Res 2003;111:59–64
37. McClatchey PM, Keller AC, Bouchard R, Knaub LA, Reusch JEB. Fully automated software for quantitative measurements of mitochondrial morphology. Mitochondrion 2016;26:58–71
38. Thomas GD, Sander M, Lau KS, Huang PL, Stull JT, Victor RG. Impaired metabolic modulation of alpha-adrenergic vasoconstriction in dystrophin-deficient skeletal muscle. Proc Natl Acad Sci U S A 1998;95:15090–15095
39. Griffith OW, Kilbourn RG. Nitric oxide synthase inhibitors: amino acids. Methods Enzymol 1996;268:375–392
40. Lee J-F, Gordon S, Estrada R, et al. Balance of S1P1 and S1P2 signaling regulates peripheral microvascular permeability in rat cremaster muscle vasculature. Am J Physiol Heart Circ Physiol 2009;296:H33–H42
41. Thompson M, Becker L, Bryant D, et al. Expression of the inducible nitric oxide synthase gene in diaphragm and skeletal muscle. J Appl Physiol (1985) 1996;81:2415–2420
42. Copp SW, Hirai DM, Schwagerl PJ, Musch TI, Poole DC. Effects of neuronal nitric oxide synthase inhibition on resting and exercising hindlimb muscle blood flow in the rat. J Physiol 2010;588:1321–1331
43. Azizi PM, Zyla RE, Guan S, et al. Clathrin-dependent entry and vesicle-mediated exocytosis define insulin transcytosis across microvascular endothelial cells. Mol Biol Cell 2015;26:740–750
44. Yuan SY. New insights into eNOS signaling in microvascular permeability. Am J Physiol Heart Circ Physiol 2006;291:H1029–H1031
45. Kurose I, Kubes P, Wolf R, et al. Inhibition of nitric oxide production. Mechanisms of vascular albumin leakage. Circ Res 1993;73:164–171
46. Rumbaut RE, Wang J, Huxley VH. Differential effects of L-NAME on rat venular hydraulic conductivity. Am J Physiol Heart Circ Physiol 2000;279:H2017–H2023
47. Predescu D, Predescu S, Shimizu J, Miyawaki-Shimizu K, Malik AB. Constitutive eNOS-derived nitric oxide is a determinant of endothelial junctional integrity. Am J Physiol Lung Cell Mol Physiol 2005;289:L371–L381
48. Le Gouill E, Jimenez M, Binnert C, et al. Endothelial nitric oxide synthase (eNOS) knockout mice have defective mitochondrial beta-oxidation. Diabetes 2007;56:2690–2696
49. Kubis N, Richer C, Domergue V, Giudicelli J-F, Lévy BI. Role of microvascular rarefaction in the increased arterial pressure in mice lacking for the endothelial nitric oxide synthase gene (eNOS3pt-/-). J Hypertens 2002;20:1581–1587
50. Natali A, Quiñones Galvan A, Pecori N, Sanna G, Toschi E, Ferrannini E. Vasodilation with sodium nitroprusside does not improve insulin action in essential hypertension. Hypertension 1998;31:632–636
51. Zeng G, Quon MJ. Insulin-stimulated production of nitric oxide is inhibited by wortmannin. Direct measurement in vascular endothelial cells. J Clin Invest 1996; 98:894–898
52. Poythress RH, Gallant C, Vetterkind S, Morgan KG. Vasoconstrictor-induced endocytic recycling regulates focal adhesion protein localization and function in vascular smooth muscle. Am J Physiol Cell Physiol 2013;305:C215–C227
53. Balon TW, Nadler JL. Evidence that nitric oxide increases glucose transport in skeletal muscle. J Appl Physiol (1985) 1997;82:359–363
54. Etgen GJ Jr., Fryburg DA, Gibbs EM. Nitric oxide stimulates skeletal muscle glucose transport through a calcium/contraction- and phosphatidylinositol-3-kinase-independent pathway. Diabetes 1997;46:1915–1919
55. Kapur S, Bédard S, Marcotte B, Côté CH, Marette A. Expression of nitric oxide synthase in skeletal muscle: a novel role for nitric oxide as a modulator of insulin action. Diabetes 1997;46:1691–1700